



Published in final edited form as:

Mol Carcinog. 2012 March ; 51(3): 280–289. doi:10.1002/mc.20844.

Green Tea Catechin Extract in Intervention of Chronic Breast Cell Carcinogenesis Induced by Environmental Carcinogens

Kusum Rathore^{1,2} and Hwa-Chain Robert Wang^{1,2,*}

¹Department of Biomedical and Diagnostic Sciences, College of Veterinary Medicine, The University of Tennessee, Knoxville, TN

²Graduate School of Genome Science and Technology, The University of Tennessee, Knoxville, TN

Abstract

Sporadic breast cancers are mainly attributable to long-term exposure to environmental factors, via a multi-year, multi-step, and multi-path process of tumorigenesis involving cumulative genetic and epigenetic alterations in the chronic carcinogenesis of breast cells from a non-cancerous stage to precancerous and cancerous stages. Epidemiologic and experimental studies have suggested that green tea components may be used as preventive agents for breast cancer control. In our research, we have developed a cellular model that mimics breast cell carcinogenesis chronically induced by cumulative exposures to low doses of environmental carcinogens. In this study, we used our chronic carcinogenesis model as a target system to investigate the activity of green tea catechin extract (GTC) at non-cytotoxic levels in intervention of cellular carcinogenesis induced by cumulative exposures to pico-molar 4-(methylnitrosamino)-1-(3-pyridyl)-1-butanone (NNK) and benzo[a]pyrene (B[a]P). We identified that GTC, at a non-cytotoxic, physiologically-achievable concentration of 2.5 µg/mL, was effective in suppressing NNK- and B[a]P-induced cellular carcinogenesis, as measured by reduction of the acquired cancer-associated properties of reduced dependence on growth factors, anchorage-independent growth, increased cell mobility, and acinar-conformational disruption. We also detected that intervention of carcinogen-induced elevation of reactive oxygen species (ROS), increase of cell proliferation, activation of the ERK pathway, DNA damage, and changes in gene expression may account for the mechanisms of GTC's preventive activity. Thus, GTC may be used in dietary and chemoprevention of breast cell carcinogenesis associated with long-term exposure to low doses of environmental carcinogens.

Keywords

breast cancer; dietary prevention; reactive oxygen species; ERK; DNA damage

INTRODUCTION

More than 70% of sporadic breast cancers are attributable to long-term exposure to environmental factors, such as chemical carcinogens; this chronic disease process involves accumulated genetic and epigenetic alterations to induce progressive carcinogenesis of breast cells from non-cancerous to precancerous and cancerous stages [1–4]. The current paradigm of experimental studies routinely uses high doses of carcinogens (micro- to millimolar concentrations) to induce cancerous cells in cultures and tumors in animals as steps in

*Correspondence to: Dr. Hwa-Chain R. Wang, Department of Biomedical and Diagnostic Sciences, College of Veterinary Medicine, University of Tennessee, 2407 River Drive, Knoxville, TN 37996, USA; Tel: +1-865-974-3846; Fax: +1-865-974-5640; hcrwang@utk.edu.

evaluating the potency of carcinogens [1,3,5]. However, considering that long-term, chronic exposure to low doses of carcinogens is responsible for human breast cancer, a high-dose approach may not be a proper way to study environmental carcinogens in human breast cancer development.

We have been developing a cellular model to mimic chronic breast cell carcinogenesis occurring with accumulated exposures to low doses of environmental carcinogens, such as 4-(methylnitrosamino)-1-(3-pyridyl)-1-butanone (NNK) and/or benzo[a]pyrene (B[a]P) [6–9]. NNK is a tobacco-specific carcinogen [10,11]. Although gastric administration of NNK into rats results in DNA-adduct formation in the mammary gland [12] and development of mammary tumors [13], NNK is not currently recognized as a mammary carcinogen. B[a]P is an environmental, dietary, and tobacco carcinogen [14–18]. Epidemiologic, animal, and cellular studies indicate that B[a]P may contribute to sporadic breast cancer development through its metabolites forming DNA-adducts causing DNA lesions [17–20]. However, the association between smoking and breast cancer is still controversial; some studies have indicated there is no influence of smoking on breast cancer incidence [21], and some studies have shown a correlation between them [22]. Recently, a study was conducted by four major Canadian agencies to address this controversy, and the results indicate that active smoking and second-hand smoke increase breast cancer risk [23]. Another recent cohort study in the United States has also shown a connection between smoking and breast cancer in post-menopausal women [24]. Thus, the role of smoking in increasing the incidence of breast cancer should be taken seriously. Our model system has successfully revealed that NNK and B[a]P, at pico-molar ranges, like those detected in patients, are able to induce non-cancerous breast epithelial MCF10A cells to increasingly acquire cancer-associated properties via cumulative exposures [6–9].

The use of green tea to increase the body's antioxidant activity is becoming increasingly popular in the Western world [25]. Animal studies show that green tea catechin extract (GTC) is able to suppress rat mammary carcinogenesis induced by 7,12-dimethylbenz[a]anthracene and N-methyl-N-nitrosourea [26,27]. Laboratory studies also have shown that GTC possesses inhibitory and apoptotic activity in human breast cancer cells in cultures [28,29]. Although they are controversial, epidemiological studies have examined the benefits of tea consumption for breast cancer prevention, and some evidence has indicated that green tea consumption may help prevent breast cancer recurrence in early stage cancers [30–32]. Thus, it is important to identify carcinogens whose induction of breast cell carcinogenesis can be intervened by green tea components to reveal targets for dietary prevention. Using our cellular model as a target, we have tested the ability of GTC at a non-cytotoxic concentration of 40 µg/mL to suppress, by more than 50%, the acquisition of cancer-associated properties induced by cumulative exposures to 100 pmol/L of B[a]P [7]. Hence, it is important to pursue an extended study to reveal the effectiveness and mechanisms of GTC in intervention of chronic breast cell carcinogenesis caused by NNK and B[a]P for developing targeted intervention of breast cell carcinogenesis.

In this study, we used our cellular model as a target and investigated the minimal concentration of GTC required for intervention of NNK- and B[a]P-induced cellular carcinogenesis. We also investigated the mechanisms for GTC in counteracting the activity of NNK and B[a]P in inducing cellular, biochemical, and molecular changes on initiation of cellular carcinogenesis.

MATERIALS AND METHODS

Cell Cultures and Reagents

MCF10A (American Type Culture Collection [ATCC], Rockville, MD) and derived cells were maintained in complete (CM) medium (1:1 mixture of DMEM and Ham's F12, supplemented with mitogenic additives including 100 ng/ml cholera enterotoxin, 10 µg/ml insulin, 0.5 µg/ml hydrocortisol, 20 ng/ml epidermal growth factor, and 5% horse serum) and supplemented with 100 units/ml penicillin and 100 µg/ml streptomycin [6–9]. All the cultures were maintained in 5% CO₂ at 37°C. Stock aqueous solutions of NNK (Chemsyn, Lenexa, KS), B[a]P (Aldrich, Milwaukee, WI), and chloromethyl-dichlorodihydro-fluorescein-diacetate (CM-H₂DCF-DA) (Invitrogen, Carlsbad, CA) were prepared in DMSO and diluted with culture medium for assays. GTC (Polyphenon-60, a mixture of polyphenolic compounds containing 60% total catechins, Sigma, St. Louis, MO) was prepared in distilled water and diluted with medium.

Induction and Suppression of Cell Carcinogenesis

Twenty-four hours after each subculturing, MCF10A cells were treated with combined NNK and B[a]P each at 100 pmol/L in the absence and presence of GTC for 48 h as one cycle of exposure for 10 cycles; cultures were subcultured every 3 d.

Cell Viability Assay

A Methyl Thiazolyl Tetrazolium (MTT) assay kit (ATCC) was used to measure cell growth and viability in cultures. Five × 10³ cells were seeded into each well of 96-well culture plates. After treatments, cultures were incubated with MTT reagent for 4 h, followed by incubation with detergent reagent for 24 h. Reduced MTT reagent in cultures was quantified with an ELISA reader (Bio-Tek, Winooski, VT).

Cell Proliferation Assay

Five × 10³ cells were seeded into each well of 96-well culture plates. After treatments, using the 5-bromo-2-deoxyuridine (BrdU) cell proliferation ELISA kit (Roche, Indianapolis, IN), cultures were labeled with BrdU for 12 h, fixed, incubated with peroxidase-conjugated BrdU-specific antibodies, and stained with the peroxidase substrate. Quantification of BrdU-labeled cells was determined with an ELISA reader (Bio-Tek).

Apoptosis Assay

An annexin-V-fluorescein isothiocyanate (FITC) apoptosis detection kit with propidium iodide (BD Biosciences, San Jose, CA) was used to detect apoptotic cell death by flow cytometry, as described previously [33]. Flow cytometric analysis was performed on the Coulter EPICS Elite Cytometer (Hialeah, FL) at the excitation and emission wavelengths of 488 and 550 nm, respectively, for FITC measurements, and at 488 and 645 nm for propidium iodide measurements. Percentage of cells undergoing apoptosis was determined using Multicycle software (Phoenix Flow System, San Diego, CA).

Reduced Dependence on Growth Factors Assay

The low-mitogen (LM) medium contained total serum and mitogenic additives reduced to 2% of the concentration formulated in CM medium as described above [7–9]. Three × 10³ cells were seeded in LM medium; growing colonies that reached 0.5 mm diameter in 10 d were counted.

Anchorage-independent Cell Growth Assay

The base layer consisted of 2% low-melting agarose (Sigma) in CM medium. Then, soft agar consisting of 0.4% low-melting agarose in a mixture (1:1) of CM medium with 3-d conditioned medium prepared from MCF10A cultures was mixed with 5×10^3 cells and plated on top of the base layer in 60-mm diameter culture dishes [7–9]; growing colonies that reached 0.1 mm diameter in 20 d were counted.

Acinar-Conformational Disruption Assay

Placed as a Matrigel base of reconstituted basement membrane in each well of 24-well culture plates was 400 μ L of growth factor-reduced Matrigel Matrix (BD Biosciences) [7, 8, 34]. Two $\times 10^3$ cells were mixed with CM medium containing 4% Matrigel and plated on top of the base layer of Matrigel. Cultures were maintained in 5% CO₂ at 37°C and were replaced with fresh CM medium containing 2% Matrigel every 3 d for 14 d. Spheroids in Matrigel were collected and overlaid with 5% agarose; then blocks of agarose-packed Matrigel spheroids were fixed in neutral-buffered formalin and embedded in paraffin for histological examination of 5-mm H&E-stained sections.

Cell Motility Assay

Cells were grown to confluence in CM medium, rinsed with PBS, and maintained in DMEM/Ham's F12 media supplemented with 2% serum for 15 h [35]. The monolayer was scratched with a 23-gauge needle (BD Biosciences) to generate wounded areas and rinsed with CM medium to remove floating cells. Cultures were maintained in CM medium, and the wounded areas were examined 6 h and 24 h after scratches. Wound healing area was calculated by using Total Lab TL100 software (Total Lab, Newcastle, NE).

Intracellular ROS Measurement

Cultures were labeled with 5 μ M CM-H₂DCF-DA for 1 h [36]. Cells were trypsinized from cultures and resuspended in PBS for analysis of ROS by flow cytometry, using a 15 mW, air-cooled argon laser to produce 488 nm light. DCF fluorescence emission was collected with a 529 nm band pass filter. The mean fluorescence intensity of 2×10^4 cells was quantified using Multicycle software (Phoenix Flow System).

Western Immunoblotting

Cell lysates were prepared in buffer (10 mM Tris-HCl, 150 mM NaCl, 1% Triton X-100, 5 mM EDTA, 10 mM sodium pyrophosphate, 10% glycerol, 0.1% Na₃VO₄, 50 mM NaF, pH 7.4) [8,9]. Protein concentration in cell lysates was measured using the BCA assay (Pierce, Rockford, IL). Equal amounts of cellular proteins were resolved by electrophoresis in 10 or 12% SDS-polyacrylamide gels for Western immunoblotting with antibodies specific to phosphorylated Mek1/2 (p-Mek1/2), Mek1/2, p-Erk1/2, p-H2AX, H2AX (Cell Signaling, Beverly, MA), Erk1/2, and β -Actin (Santa Cruz, Santa Cruz, CA). Antigen-antibody complexes on filters were detected by the Supersignal chemiluminescence kit (Pierce).

Gene Expression Study with Microarrays

MCF10A cells were treated with combined NNK and B[a]P each at 100 pmol/L in the absence or presence of 40 μ g/mL of GTC for 24 h. Total RNA was isolated from cultures using the Absolutely RNA kit (Stratagene, La Jolla, CA). RNA quality and integrity were determined using an Agilent 2100 Bioanalyzer (Agilent, Palo Alto, CA). High-quality RNA, with an RNA Integrity Number of >7.0 and an A260/280 absorbance ratio of >1.8, was used for studies. Detection of gene expression was completed through a purchased service using the Human OneArray, which contains 29,187 human genome probes and 1088 experimental control probes formed as 60-mer sense-strand DNA elements (PhalanxBio, Palo Alto, CA).

All experiments were performed in duplicate; RNA was prepared from two independent cultures for each experiment. The data was analyzed using Array Studio Online (OmicSoft, Morrisville, NC). The relative gene expression levels in carcinogen- and GTC-treated cultures were normalized with levels in their counterpart, parental MCF10A cells and then were reciprocally compared to detect differentially expressed genes in GTC- and carcinogen (only)-treated cultures versus carcinogen-treated cultures.

Reverse Transcription PCR

One μg of total RNA isolated from cultures using the Absolutely RNA kit (Stratagene) was reverse transcribed to cDNA using a Versoc DNA Kit (Thermo Scientific, Waltham, MA). The resulting cDNAs were subjected to PCR for COX17 (forward: 5'-TCTAATTGAGGCCCAAGG-3'; reverse: 5'-ATTCACACAGCAGACCACCA-3'), TNFRSF8 (forward: 5'-AAACCGCTCAGATGTTTTGG-3'; reverse: 5'-TGATGCAGAGACACCCACTC-3'), S100P (forward: 5'-TCCTGCAGAGTGGAAAAGAC-3'; reverse: 5'-TAGGGGAATAATTGCCAACA-3'), ATM (forward: 5'-ACTGCCAAGGACAAATGAGG-3'; reverse: 5'-TGAGCAACTGAGTGGCAAAC-3'), and β -Actin (forward: 5'-GGACTTCGAGCAAGAGATGG-3'; reverse: 5'-AGCACTGTGTTGGCGTACAG-3'). PCR was carried out as follows: 1 cycle at 95°C for 2 min, 45 cycles at 95°C for 30 s and 58°C for 45 s, and the final extension of 1 cycle at 72°C for 30 s. PCR products were electrophoresed on 2% agarose gel and visualized after ethidium bromide staining.

Statistical Analysis

To statistically verify the suppression of NNK- and B[a]P-induced carcinogenesis by GTC, one-way analysis of variance (ANOVA) test was used to establish significant difference among the various treatment groups at $P < 0.01$, followed by Duncan's Multiple Range Test. Statistical significance of all the other studies was analyzed by Student t test ($P \leq 0.05$) and α levels were adjusted by the Simes method [37].

RESULTS AND DISCUSSION

Determination of GTC Cytotoxicity

Considering the side-effects resulting from long-term use of anticancer agents in intervention of cellular carcinogenesis, use of non-cytotoxic levels of dietary components has to be adopted into strategies for cancer prevention. To determine the cytotoxicity of GTC to non-cancerous breast epithelial cells, we investigated the biological effects of GTC at various concentrations on viability, proliferation, and cell death of MCF10A cells. We detected cytotoxic activity of GTC at 100 $\mu\text{g}/\text{mL}$, but not at 0.5, 2.5, 10, and 40 $\mu\text{g}/\text{mL}$, in reducing cell viability (Figure 1A), inhibiting cell proliferation (1B), or inducing apoptotic cell death (1C). Accordingly, GTC at 0.5, 2.5, 10, and 40 $\mu\text{g}/\text{mL}$ was non-cytotoxic to MCF10A cells.

GTC Suppression of NNK- and B[a]P-induced Carcinogenesis

In our chronic carcinogenesis model, cumulative exposures of MCF10A cells to pico-molar NNK and B[a]P result in progressive acquisition of various cancer-associated properties [7–9]. Using cancer-associated properties as target endpoints, we investigated the activity of GTC in suppression of NNK- and B[a]P-induced cellular carcinogenesis. A lack of growth factors causes normal cells to become growth-arrested in the cell cycle and to commit apoptosis; however, aberrantly-increased cell survivability acquired to reduce dependence on growth factors can lead cells to tumorigenic transformation [38–40]. Cell adhesion to extracellular matrixes is important for cell survival in a multi-cell environment; aberrantly-

increased cell survivability acquired to promote anchorage-independent growth can render cells into tumorigenic transformation [41,42]. Cancerous cells acquire an increased mobility compared with their normal counterpart cells [43]. MCF10A cells were exposed to NNK combined with B[a]P in the presence of GTC at 0, 0.5, 2.5, 10, and 40 $\mu\text{g}/\text{mL}$ for 10 cycles, resulting in NB, NB/G-0.5, NB/G-2.5, NB/G-10, and NB/G-40 cell lines, respectively. We detected that GTC at 2.5, 10, and 40 $\mu\text{g}/\text{mL}$ significantly suppressed NNK- and B[a]P-induced acquisition of the cancer-associated property of reduced dependence on growth factors to approximately 20, 40, and 75%, respectively (Figure 2A-1), as well as anchorage-independent growth to approximately 20, 50, and 80%, respectively (2B-1). Not only the numbers but also sizes of cell colonies were suppressed by GTC (Figure 2A-2 and 2B-2). Using the scratch/wound assay [35], we detected that NB cells acquired high mobility to heal the wounded area in 24 h; in contrast, parental MCF10A cells did not heal the wounded area; and NB/G-0.5, NB/G-2.5, NB/G-10, and NB/G-40 cells showed various abilities to heal the wounded areas (Figure 2C-1). Thus, co-exposure to GTC significantly reduced NNK- and B[a]P-induced acquisition of the cancer-associated property of increased cell mobility in a dose-dependent manner (Figure 2C-2).

In addition, both acinar structures with a hollow lumen and apicobasally polarized cells are important characteristics found in glandular epithelia in vivo; the disruption of an intact glandular structure is a hallmark of epithelial cancer even at precancerous stages [44,45]. As shown in our previous studies [7–9], parental MCF10A cells mainly formed regular, round spheroids on Matrigel cultures, and NNK- and B[a]P-exposed cells formed both regular and irregular spheroids. Counting the regular and irregular spheroids in these cultures verified the ability of GTC at 2.5, 10, and 40 $\mu\text{g}/\text{mL}$ to significantly suppress NNK- and B[a]P-induced development of irregular spheroids to approximately 10, 45, and 65%, respectively (Figure 2D-1). Histological examination revealed a hollow lumen and apicobasal polarization in regular spheroids of MCF10A cells and GTC-protected, carcinogen-exposed cells (NB/G-40) as well as the loss of apicobasal polarity and filling of the luminal space in irregular spheroids of NNK- and B[a]P-exposed cells (NB) and NB/G-40 cells on Matrigel (Figure 2D-2). These results indicated that GTC was able to protect MCF10A cells from acquiring the cancer-associated property of acinar-conformational disruption induced by NNK and B[a]P in a dose-dependent manner.

Analysis of all these results together indicated that GTC at 2.5, 10, and 40 $\mu\text{g}/\text{mL}$ was effective to significantly suppress NNK- and B[a]P-induced cellular carcinogenesis quantitatively and qualitatively. Clinical and animal studies showed an achievable plasma level of GTC at 4 $\mu\text{g}/\text{mL}$ [46–49]. Therefore, GTC at 2.5 $\mu\text{g}/\text{mL}$ can be bio-availably achieved for dietary intervention and chemoprevention of breast cell carcinogenesis associated with long-term exposure to environmental carcinogens.

MCF10A cells repeatedly treated with combined NNK and B[a]P each at 100 pmol/L for 10 cycles acquired various cancer-associated properties but did not acquire tumorigenicity to develop any detectable xenograft tumors in immunodeficient nude mice (data not shown). It has been shown that NNK is able to induce mammary tumors in rats [13], and it is recognized that exposure to B[a]P contributes to sporadic breast cancer development [17–20]. Although NNK and B[a]P are recognized as precancerous breast carcinogens in our model, whether additional exposures to NNK and B[a]P may induce cellular tumorigenicity remains to be determined. Thus, our model is able to detect precancerous carcinogenesis of breast cells and identify preventive agents to intervene in precancerous breast cell carcinogenesis for early prevention of breast cancer associated with long-term exposure to low doses of environmental and tobacco carcinogens.

GTC Suppression of Carcinogen-induced ROS, Cell Proliferation, the ERK Pathway, and H2AX Phosphorylation

Short-term exposure of MCF10A cells to the B[a]P metabolites B[a]P-quinones at 10 $\mu\text{mol/L}$ induces ROS [50]. Short-term exposure of normal human bronchial epithelial cells to NNK at 1–5 $\mu\text{mol/L}$ induces cell proliferation [51]. It has been postulated that ROS elevation and increased proliferation may promote cell susceptibility to DNA damage induced by carcinogens, contributing to cellular carcinogenesis [52,53]. However, it is not clear whether MCF10A cell carcinogenesis induced by cumulative exposures to NNK and B[a]P at 100 pmol/L is contributed by ROS elevation, proliferation, and DNA damage during each exposure. To address this question and to pursue the mechanisms for GTC in counteracting the activity of NNK and B[a]P in initiation of cellular carcinogenesis, we studied the activity of GTC in modulation of NNK- and B[a]P-induced ROS elevation, cell proliferation, proliferation-associated signaling pathways, and DNA damage. As shown in Figure 3, treatment with NNK and B[a]P for 24 h induced ROS elevation (A), cell proliferation (B), activation of the ERK pathway (indexed by phosphorylation of Mek1/2 and Erk1/2) [54] (C), and DNA damage (indexed by phosphorylation of H2AX on serine-139) [55] (C). Co-treatment with GTC at 2.5, 10, and 40 $\mu\text{g/mL}$ resulted in a dose-dependent reduction of these carcinogen-induced biological and biochemical outcomes. Accordingly, suppression of carcinogen-induced ROS elevation, cell proliferation, ERK activation, and DNA damage may account for the mechanism of GTC in intervention of cellular carcinogenesis. However, the targets involved in ROS elevation, cell proliferation, ERK activation, and DNA damage for GTC suppression of NNK- and B[a]P-initiated carcinogenesis are to be identified.

GTC Intervention of Carcinogen-induced Gene Expression

To further our investigation of GTC activity in intervention of NNK- and B[a]P-initiated carcinogenesis, we used cDNA microarrays to detect differentially regulated genes that were changed in carcinogen-treated cells but whose changes were suppressed by GTC. Initially, we identified genes whose expressions were changed in carcinogen-treated cells compared to their counterpart expression levels in untreated cells. After normalization, more than 11,000 genes were detectably expressed in these cells. Filtering with the *t* test ($P < 0.05$) revealed 479 differentially expressed genes in carcinogen-treated cells, more than 2-fold over counterpart expression in untreated, counterpart cells. Subsequently, we identified genes whose expressions were associated with ROS elevation, cell proliferation, the ERK pathway activation, and DNA damage, but were not induced in GTC- and carcinogen-treated cells. As listed in Table 1, we detected that three genes (BAX, COX17, and MRPL41) associated with ROS elevation, four genes (B4GALT1, BARHL1, BOLA3, and MT1E) associated with cell proliferation, two genes (S100P and SPRR1B) associated with ERK pathway activation, and two genes (ATM and PER1) associated with DNA damage were up-regulated in carcinogen-treated cells but their up-regulations were suppressed in GTC- and carcinogen-treated cells; in addition, one gene (TNFRSF8) associated with negative regulation of cell proliferation was down-regulated in carcinogen-treated cells but not down-regulated in GTC- and carcinogen-treated cells. To further validate microarray results with an independent method, we arbitrarily chose a gene from each category for reverse transcription PCR semi-quantification to measure relative gene expression levels in cells treated with carcinogens and/or GTC. As shown in Figure 4, gene expression of COX17, S100P and ATM, which were associated with ROS elevation, ERK pathway activation, and DNA damage, respectively, were increased by NNK and B[a]P treatment; but NNK- and B[a]P-increased expression of these genes was significantly reduced by co-treatment with GTC. In contrast, TNFRSF8 gene expression associated with cell proliferation was reduced in cells treated with NNK and B[a]P and up-regulated in cultures treated with GTC alone or GTC and carcinogens. The PCR results were consistent with

microarray data. Accordingly, expression of these genes may be considered as a molecular target endpoint for GTC intervention of NNK- and B[a]P-initiated cellular carcinogenesis. However, their roles in carcinogen-induced ROS elevation, cell proliferation, ERK activation, and DNA damage and GTC-induced suppression of carcinogenesis are to be identified.

Our model presents unique features of chronic induction of breast cell carcinogenesis by cumulative exposures to carcinogens, high sensitivity to detect low levels of carcinogens, and measurable target endpoints. Applying this cellular model as a target will accelerate the identification of dietary components for the formulation of combined supplements that can effectively reduce the health risk of human cancers from long-term exposure to carcinogens present in environmental pollution.

Acknowledgments

We are grateful to Ms. M. Bailey for textual editing of the manuscript. We thank Ms. DJ Trent for technique support in flow cytometric analysis of ROS and apoptosis. This study was supported by a grant from the University of Tennessee, College of Veterinary Medicine, Center of Excellence in Livestock Diseases and Human Health (to H-C.R. W.) and the National Institutes of Health (CA125795 and CA129772 [H-C.R. W.]).

Abbreviations

ATCC	American Type Culture Collection
ANOVA	a one-way analysis of variance
BrdU	5-bromo-2'-deoxyuridine
B[a]P	benzo[a]pyrene
CM-H₂DCF-DA	chloromethyl-dichlorodihydrofluorescein-diacetate
CM medium	complete MCF10A medium
FITC	fluorescein isothiocyanate
GTC	green tea catechin extract
LM medium	low-mitogen medium
MTT	methyl thiazolyl tetrazolium
NNK	4-(methylnitrosamino)-1-(3-pyridyl)-1-butanone
ROS	reactive oxygen species

References

1. Kelloff, GJ.; Hawk, ET.; Sigman, CC. Cancer chemoprevention: Strategies for cancer chemoprevention. Vol. 2. Totowa, New Jersey: Human Press; 2005.
2. DeBruin LS, Josephy PD. Perspectives on the chemical etiology of breast cancer. *Environ Health Perspect.* 2002; 1(110 Suppl):119–128. [PubMed: 11834470]
3. Hecht SS. Tobacco smoke carcinogens and breast cancer. *Environ Mol Mutagen.* 2002; 39:119–126. [PubMed: 11921179]
4. Guengerich FP. Metabolism of chemical carcinogens. *Carcinogenesis.* 2000; 21:345–515. [PubMed: 10688854]
5. Mehta RG. Experimental basis for the prevention of breast cancer. *Eur J Cancer.* 2000; 36:1275–1282. [PubMed: 10882866]

6. Mei J, Hu H, McEntee M, Plummer H III, Song P, Wang HCR. Transformation of noncancerous human breast epithelial cell MCF10A induced by the tobacco-specific carcinogen NNK. *Breast Cancer Res Treat.* 2003; 79:95–105. [PubMed: 12779086]
7. Siriwardhana N, Wang HCR. Precancerous carcinogenesis of human breast epithelial cells by chronic exposure to benzo[a]pyrene. *Mol Carcinogenesis.* 2008; 47:338–348.
8. Siriwardhana N, Choudhary S, Wang HCR. Precancerous model of human breast epithelial cells induced by the tobacco-specific carcinogen NNK for prevention. *Breast Cancer Res Treat.* 2008; 109:427–441. [PubMed: 17653854]
9. Song X, Siriwardhana N, Rathore K, Lin D, Wang HCR. Grape seed proanthocyanidin suppression of breast cell carcinogenesis induced by chronic exposure to combined 4-(methylnitrosamino)-1-(3-pyridyl)-1-butanone and benzo[a]pyrene. *Mol Carcinogenesis.* 2010; 49:450–463.
10. Hecht SS. Recent studies on mechanisms of bioactivation and detoxification of 4-(methylnitrosamino)-1-(3-pyridyl)-1-butanone (NNK), a tobacco specific lung carcinogen. *Crit Rev Toxicol.* 1996; 26:163–181. [PubMed: 8688159]
11. Hecht SS. Tobacco smoke carcinogens and lung cancer. *J Natl Cancer Inst.* 1999; 91:1194–1210. [PubMed: 10413421]
12. Wu Z, Upadhyaya P, Carmella SG, et al. Disposition of 4-(methylnitrosamino)-1-(3-pyridyl)-1-butanone (NNK) and 4-(methylnitrosamino)-1-(3-pyridyl)-1-butanol (NNAL) in bile duct-cannulated rats: Stereoselective metabolism and tissue distribution. *Carcinogenesis.* 2002; 23:171–179. [PubMed: 11756238]
13. Chhabra SK, Anderson LM, Perella C, et al. Coexposure to ethanol with N-nitrosodimethylamine or 4-(Methylnitrosamino)-1-(3-pyridyl)-1-butanone during lactation of rats: marked increase in O(6)-methylguanine-DNA adducts in maternal mammary gland and in suckling lung and kidney. *Toxicol Appl Pharmacol.* 2000; 169:191–200. [PubMed: 11097872]
14. Grover PL, Martin FL. The initiation of breast and prostate cancer. *Carcinogenesis.* 2002; 23:1095–1102. [PubMed: 12117765]
15. Wogan GN, Hecht SS, Felton JS, Conney AH, Loeb LA. Environmental and chemical carcinogenesis. *Semin Cancer Biol.* 2004; 14:473–486. [PubMed: 15489140]
16. Rubin H. Synergistic mechanisms in carcinogenesis by polycyclic aromatic hydrocarbons and by tobacco smoke: A bio-historical perspective with updates. *Carcinogenesis.* 2001; 22:1903–1930. [PubMed: 11751421]
17. Rundle A, Tang D, Hibshoosh H, et al. The relationship between genetic damage from polycyclic aromatic hydrocarbons in breast tissue and breast cancer. *Carcinogenesis.* 2000; 21:1281–1289. [PubMed: 10874004]
18. Morris JJ, Seifter E. The role of aromatic hydrocarbons in the genesis of breast cancer. *Med Hypotheses.* 1992; 38:177–184. [PubMed: 1513270]
19. Shou M, Harvey RG, Penning TM. Reactivity of benzo[a]pyrene-7,8-dione with DNA. Evidence for the formation of deoxyguanosine adducts. *Carcinogenesis.* 1993; 14:475–482. [PubMed: 8384091]
20. Caruso JA, Reiners JJ Jr, Emond J, et al. Genetic alteration of chromosome 8 is a common feature of human mammary epithelial cell lines transformed in vitro with benzo[a]pyrene. *Mutat Res.* 2001; 473:85–99. [PubMed: 11166028]
21. Prescott J, Ma H, Bernstein L, Ursin G. Cigarette smoking is not associated with breast cancer risk in young women. *Cancer Epidemiol Biomarkers Prev.* 2007; 16:620–622. [PubMed: 17372262]
22. Terry PD, Rohan TE. Cigarette smoking and the risk of breast cancer in women: a review of the literature. *Cancer Epidemiol Biomarkers Prev.* 2002; 11:953–971. [PubMed: 12376493]
23. Johnson KC, Miller AB, Collishaw NE, et al. Active smoking and secondhand smoke increase breast cancer risk: the report of the Canadian Expert Panel on Tobacco Smoke and Breast Cancer Risk (2009). *Tobacco Control.* 2011; 20:e2. [PubMed: 21148114]
24. Luo J, Margolis KL, Wactawski-Wende J, et al. Association of active and passive smoking with risk of breast cancer among postmenopausal women: a prospective cohort study. *BMJ.* 2010; 342:1–8.
25. Zaveri NT. Green tea and its polyphenolic catechins: Medicinal uses in cancer and noncancer applications. *Life Sciences.* 2006; 78:2073–2080. [PubMed: 16445946]

26. Kavanagh KT, Hafer LJ, Kim DW, et al. Green tea extracts decrease carcinogen-induced mammary tumor burden in rats and rate of breast cancer cell proliferation in culture. *J Cell Biochem.* 2001; 82:387–398. [PubMed: 11500915]
27. Roomi MW, Roomi NW, Ivanov V, Kalinovskiy T, Niedzwiecki A, Rath M. Modulation of N-methyl-N-nitrosourea induced mammary tumors in Sprague-Dawley rats by combination of lysine, proline, arginine, ascorbic acid and green tea extract. *Breast Cancer Res.* 2005; 7:291–295.
28. Thangapazham RL, Singh AK, Sharma A, Warren J, Gaddipati JP, Maheshwari RK. Green tea polyphenols and its constituent epigallocatechin gallate inhibits proliferation of human breast cancer cells in vitro and in vivo. *Cancer Lett.* 2007; 245:232–241. [PubMed: 16519995]
29. Sartippour MR, Heber D, Ma J, Lu Q, Go VL, Nguyen M. Green tea and its catechins inhibit breast cancer xenografts. *Nutr Cancer.* 2001; 40:149–156. [PubMed: 11962250]
30. Bagchi, D.; Preuss, HG. *Phytopharmaceuticals in cancer chemoprevention.* Boca Raton, Florida: CRC Press; 2005.
31. Seely D, Mills EJ, Wu P, Verma S, Guyatt GH. The effects of green tea consumption on incidence of breast cancer and recurrence of breast cancer: A systematic review and meta-analysis. *Integr Cancer Ther.* 2005; 4:144–155. [PubMed: 15911927]
32. Boehm K, Borrelli F, Ernst E, et al. Green tea (*Camellia sinensis*) for the prevention of cancer. *Cochrane Database Syst.* 2009; 3:CD005004.
33. Choudhary S, Rathore K, Wang HCR. Differential induction of reactive oxygen species through Erk1/2 and Nox-1 by FK228 for selective apoptosis of oncogenic H-Ras-expressing human urinary bladder cancer J82 cells. *J Cancer Res Clin Oncol.* 2011; 137:471–480. [PubMed: 20473523]
34. Debnath J, Muthuswamy SK, Brugge JS. Morphogenesis and oncogenesis of MCF-10A mammary epithelial acini grown in three-dimensional basement membrane cultures. *Methods.* 2003; 30:256–268. [PubMed: 12798140]
35. Lipton A, Klinger I, Paul D, Holley RW. Migration of mouse 3T3 fibroblasts in response to a serum factor. *Proc Natl Acad Sci USA.* 1971; 11:2799–2801. [PubMed: 5288259]
36. Trachootham D, Zhou Y, Zhang H, et al. Selective killing of oncogenically transformed cells through a ROS-mediated mechanism by β -phenylethyl isothiocyanate. *Cancer Cell.* 2006; 10:241–252. [PubMed: 16959615]
37. Simes RJ. An improved Bonferroni procedure for multiple tests of significance. *Biometrika.* 1986; 73:751–754.
38. Hanahan D, Weinberg RA. The hallmarks of cancer. *Cell.* 2000; 100:57–70. [PubMed: 10647931]
39. Campisi J, Morreo G, Pardee AB. Kinetics of G1 transit following brief starvation for serum factors. *Exp Cell Res.* 1984; 152:459–466. [PubMed: 6373328]
40. Larsson O, Zetterberg A, Engstrom W. Consequences of parental exposure to serum-free medium for progeny cell division. *J Cell Sci.* 1985; 75:259–268. [PubMed: 4044676]
41. Valentijn AJ, Zouq N, Gilmore AP. Anokis. *Biochem Soc Trans.* 2004; 32:421–425. [PubMed: 15157151]
42. Reddig PJ, Juliano RL. Clinging to life: Cell to matrix adhesion and cell survival. *Cancer Metastasis Rev.* 2005; 24:425–439. [PubMed: 16258730]
43. Madsen CD, Sahai E. Cancer dissemination-lessons from leukocytes. *Dev Cell.* 2010; 1:13–26. [PubMed: 20643347]
44. Debnath J, Muthuswamy SK, Brugge JS. Morphogenesis and oncogenesis of MCF-10A mammary epithelial acini grown in three-dimensional basement membrane cultures. *Methods.* 2003; 30:256–268. [PubMed: 12798140]
45. Debnath J, Brugge JS. Modelling glandular epithelial cancers in three-dimensional cultures. *Nat Rev Cancer.* 2005; 5:675–688. [PubMed: 16148884]
46. Lee MJ, Maliakal P, Chen L, et al. Pharmacokinetics of tea catechins after ingestion of green tea and (-)-epigallocatechin-3-gallate by humans: Formation of different metabolites and individual variability. *Cancer Epidemiol Biomarkers Prev.* 2002; 11:1025–1032. [PubMed: 12376503]
47. Maiani G, Serafini M, Salucci M, Azzini E, Ferro-Luzzi A. Application of a new high-performance liquid chromatographic method for measuring selected polyphenols in human plasma. *J Chromatogr B Biomed Sci Appl.* 1997; 692:311–317. [PubMed: 9188819]

48. Lambert JD, Lee MJ, Diamond L, et al. Dose-dependent levels of epigallocatechin-3-gallate in human colon cancer cells and mouse plasma and tissues. *Drug Metab Dispos.* 2006; 34:8–11. [PubMed: 16204466]
49. Van het Hof KH, Kivits GA, Weststrate JA, Tijburg LB. Bioavailability of catechins from tea: the effect of milk. *Eur J Clin Nutr.* 1998; 52:356–359. [PubMed: 9630386]
50. Shi H, Timmins G, Monske M, et al. Evaluation of spin trapping agents and trapping conditions for detection of cell-generated reactive oxygen species. *Arch Biochem Biophys.* 2005; 437:59–68. [PubMed: 15820217]
51. Ho YS, Chen CH, Wang YJ, et al. Tobacco-specific carcinogen 4-(methylnitrosamino)-1-(3-pyridyl)-1-butanone (NNK) induces cell proliferation in normal human bronchial epithelial cells through NF κ B activation and cyclin D1 up-regulation. *Toxicol Appl Pharmacol.* 2005; 205:133–148. [PubMed: 15893541]
52. Cooke MS, Evans MD, Dizdaroglu M, Lunec J. Oxidative DNA damage: mechanisms, mutation, and disease. *FASEB J.* 2003; 10:1195–1214. [PubMed: 12832285]
53. Preston-Martin S, Pike MC, Ross RK, Henderson BE. Epidemiologic evidence for the increased cell proliferation model of carcinogenesis. *Environ Health Perspect.* 1993; 5:137–138. [PubMed: 8013400]
54. Cobb MH, Hepler JE, Cheng M, Robbins D. The mitogen-activated protein kinases, ERK1 and ERK2. *Semin Cancer Biol.* 1994; 5:261–268. [PubMed: 7803762]
55. Rogakou EP, Pilch DR, Orr AH, Ivanova VS, Bonner WM. DNA double-stranded breaks induce histone H2AX phosphorylation on serine 139. *J Biol Chem.* 1998; 10:5858–5868. [PubMed: 9488723]
56. Yoo YA, Kim MJ, Park JK, et al. Mitochondrial ribosomal protein L41 suppresses cell growth in association with p53 and p27Kip1. *Mol Cell Biol.* 2005; 25:6603–6616. [PubMed: 16024796]
57. Remacle C, Coosemans N, Jans F, Hanikenne M, Motte P, Cardol P. Knock-down of the COX3 and COX17 gene expression of cytochrome c oxidase in the unicellular green alga *Chlamydomonas reinhardtii*. *Plant Mol Biol.* 2010; 74:223–233. [PubMed: 20700628]
58. Trabosh VA, Daher A, Divito KA, Amin K, Simbulan-Rosenthal CM, Rosenthal DS. UVB upregulates the bax promoter in immortalized human keratinocytes via ROS induction of Id3. *Exp Dermatol.* 2009; 18:387–395. [PubMed: 19054058]
59. Wu Y, Siadaty MS, Berens ME, Hampton GM, Theodorescu D. Overlapping gene expression profiles of cell migration and tumor invasion in human bladder cancer identify metallothionein 1E and nicotinamide N-methyltransferase as novel regulators of cell migration. *Oncogene.* 2008; 27:6679–6689. [PubMed: 18724390]
60. Wang DY, Fulthorpe R, Liss SN, Edwards EA. Identification of estrogen-responsive genes by complementary deoxyribonucleic acid microarray and characterization of a novel early estrogen-induced gene: EEIG1. *Mol Endocrinol.* 2004; 18:402–411. [PubMed: 14605097]
61. Kasai T, Inoue M, Koshiha S, et al. Solution structure of a BOLA-like protein from *Mus musculus*. *Protein Sci.* 2004; 13:545–548. [PubMed: 14718656]
62. Li S, Qiu F, Xu A, Price SM, Xiang M. Barhl1 regulates migration and survival of cerebellar granule cells by controlling expression of the neurotrophin-3 gene. *J Neurosci.* 2004; 24:3104–3114. [PubMed: 15044550]
63. Nishikori M, Ohno H, Haga H, Uchiyama T. Stimulation of CD30 in anaplastic large cell lymphoma leads to production of nuclear factor- κ B p52, which is associated with hyperphosphorylated Bcl-3. *Cancer Sci.* 2005; 96:487–497. [PubMed: 16108830]
64. Fuentes MK, Nigavekar SS, Arumugam T, et al. RAGE activation by S100P in colon cancer stimulates growth, migration, and cell signaling pathways. *Dis Colon Rectum.* 2007; 50:1230–1240. [PubMed: 17587138]
65. Reddy SP, Adiseshaiah P, Shapiro P, Vuong H. BMK1 (ERK5) regulates squamous differentiation marker SPRR1B transcription in Clara-like H441 cells. *Am J Respir Cell Mol Biol.* 2002; 27:64–70. [PubMed: 12091247]
66. Gery S, Komatsu N, Baldjyan L, Yu A, Koo D, Koeffler HP. The circadian gene *per1* plays an important role in cell growth and DNA damage control in human cancer cells. *Mol Cell.* 2006; 22:375–382. [PubMed: 16678109]

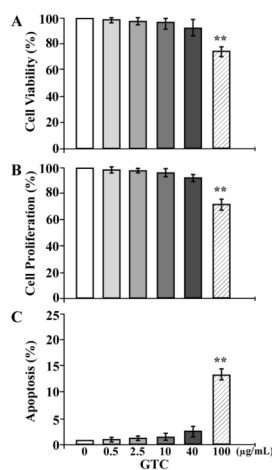


Figure 1.

Determination of GTC cytotoxicity. MCF10A cells were treated with 0, 0.5, 2.5, 10, 40, and 100 µg/mL of GTC for 48 h. (A) Quantification of cell viability was determined with an MTT assay kit, and relative cell viability was normalized by the value determined in untreated counterpart cells, set as 100%. (B) Cell proliferation was determined; relative cell growth rate was normalized by the value of BrdU detected in untreated cells, set as 100%. (C) Apoptotic cell population (%) was measured by flow cytometry with an Annexin-V-FITC Apoptosis Detection Kit. Columns, mean of triplicates; bars, SD. The Student *t* test was used to compare the control with each of the treatments to analyze statistical significance and *P* values adjusted for multiple comparisons using the Simes method, indicated by ** $P < 0.01$. All results are representative of three independent experiments.

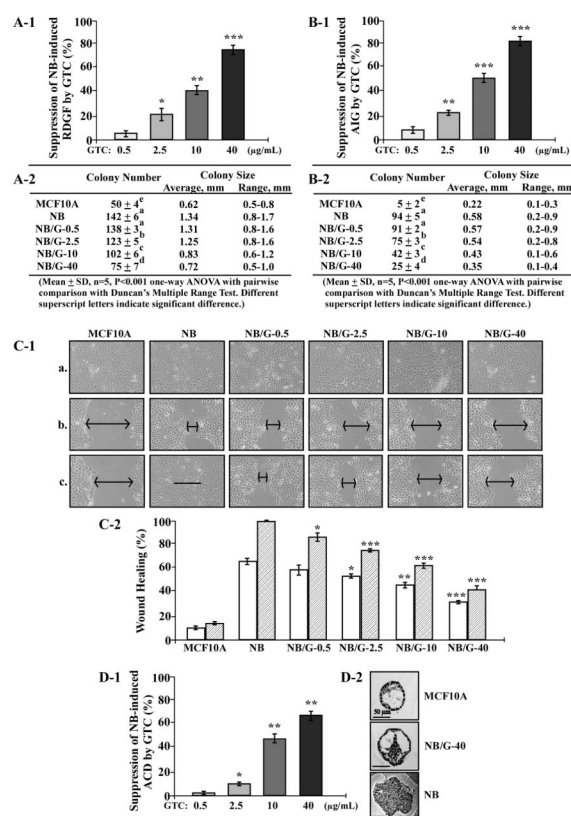
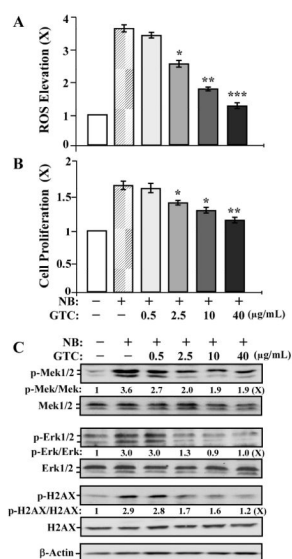


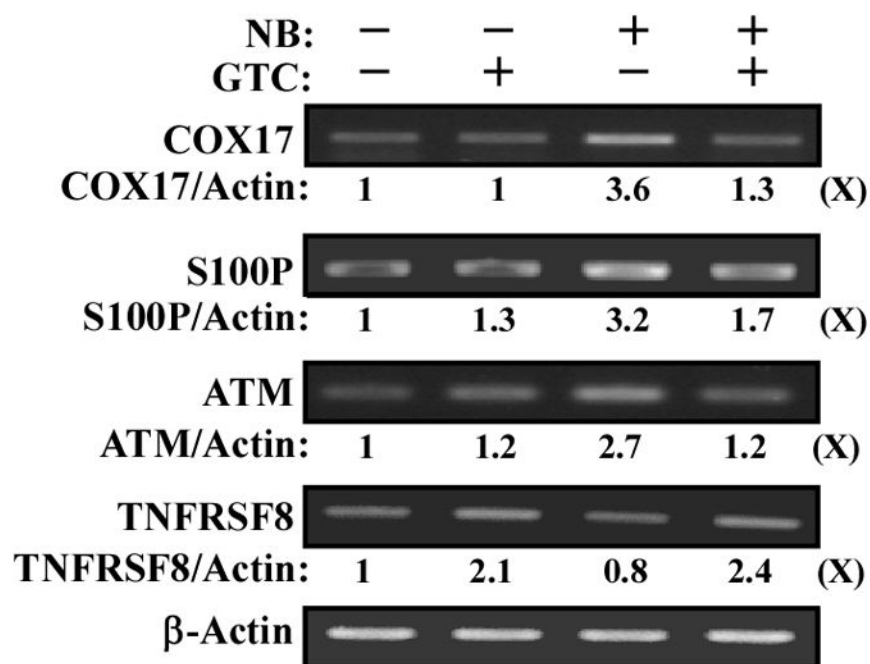
Figure 2.

GTC suppression of cellular carcinogenesis. MCF10A cells were exposed to NNK combined with B[a]P each at 100 pmol/L in the presence of GTC at 0, 0.5, 2.5, 10, and 40 μg/mL for 10 cycles, resulting in NB, NB/G-0.5, NB/G-2.5, NB/G-10, and NB/G-40 cell lines, respectively. (A-1 and A-2) To detect suppression effectivity of GTC on cellular acquisition of reduced dependence on growth factors (RDGF), cells were then seeded and maintained in LM medium for 10 d. Cell colonies (≥ 0.5 mm diameter) were stained and counted. (B-1 and B-2) To detect suppression effectivity of GTC on cellular acquisition of anchorage-independent growth (AIG), cells were seeded in soft-agar for 20 d. Colonies (≥ 0.1 mm diameter) were counted. The percentage of suppression effectivity of GTC at various concentrations on NB-induced RDGF (A-1) and AIG (B-1) were calculated by: $\{1 - [(\# \text{ of NB/G-induced cell colonies}) / (\# \text{ of MCF10A cell colonies})] \} \div [(\# \text{ of NB-induced cell colonies}) / (\# \text{ of MCF10A cell colonies})] \times 100$. Columns, mean of triplicates; bars, SD. The Student *t* test was used to compare the control with each treatment to analyze statistical significance and *P* values adjusted for multiple comparisons using the Simes method, indicated by * *P* < 0.05, ** *P* < 0.01, *** *P* < 0.001. (A-2 and B-2) colony numbers, average colony size, and range of colony size were determined in A-1 and B-1, respectively. Mean colony numbers in each treatment were analyzed by one-way ANOVA at *P* < 0.01 to indicate significant difference in number of colonies in various treatments. To further determine significant difference between individual treatments, a pairwise analysis of variables was performed using the Duncan multiple range test. Significant differences at *P* < 0.01 between treatments are labeled with different superscript letters (a, b, c, d, and e); treatments labeled with the same superscript letters indicate no significant difference. (C-1 and C-2) To detect suppression effectivity of GTC on cellular acquisition of increased cell mobility, cells were seeded in CM medium and grown to confluence (a). A linear area of cell layer was removed from each culture with a 23-gauge needle to produce wounded

cultures, and the wounded areas were examined ($\times 100$ magnification) 6 h (**b**) and 24 h (**c**) after wounding. Arrows indicate width of wounded areas. Results are representative of three independent experiments. (C-2) To calculate the wound healing area, the area not healed by the cells was subtracted from total area of initial wound to calculate the wound healing area at time intervals of 6 h (white columns) and 24 h (hatched columns). (D-1 and D-2) To detect suppression effectivity of GTC on cellular acquisition of acinar-conformation disruption (ACD), cells were seeded on Matrigel for 12 d. Regular and irregular spheroids in each Matrigel culture were counted; and then the percentage of irregular spheroids in each culture was calculated. The value of the suppression effectivity of GTC on carcinogen-induced formation of irregular spheroids was calculated by: $\{[(\% \text{ of NB-induced irregular spheroid population}) (\% \text{ of NB/G-induced irregular spheroid population})] \div [(\% \text{ of NB-induced irregular spheroid population}) (\% \text{ of irregular spheroid population in MCF10A cultures})]\} \times 100 (\%)$. *Columns*, mean of triplicates; *bars*, SD. The Student *t* test was used to compare the control with each treatment to analyze statistical significance. *P* values were adjusted for multiple comparisons using the Simes method, indicated by * $P < 0.05$, ** $P < 0.01$, *** $P < 0.001$. All results are representative of three independent experiments. (D-2) Histological examination revealed acinar features of typical regular spheroids of MCF10A, regular spheroids of NB/G-40, and irregular spheroids of NB and NB/G-40 cells on Matrigel. Bars indicate 50 μm .

**Figure 3.**

GTC suppression of carcinogen-induced ROS elevation, cell proliferation, the ERK pathway, and phosphorylation of H2AX. MCF10A cells were treated with combined NNK and B[a]P (NB) each at 100 pmol/L in the presence of 0, 0.5, 2.5, 10, and 40 µg/mL of GTC for 24 h. (A) ROS levels were measured with CM-H₂DCF-DA labeling; relative level of ROS, as fold induction (X, arbitrary unit), was normalized by the level determined in untreated counterpart cells, set as 1. (B) Cell proliferation was determined; relative cell growth rate was normalized by the value of BrdU detected in untreated counterpart cells, set as 1. Columns, mean of triplicates; bars, SD. The Student *t* test was used to compare the control with each treatment to analyze statistical significance and *P* values adjusted for multiple comparisons using the Simes method, indicated by * *P* < 0.05, ** *P* < 0.01, *** *P* < 0.001. (C) Cell lysates were prepared and analyzed by Western immunoblotting to detect levels of phosphorylated Mek1/2 (p-Mek1/2), Mek1/2, p-Erk1/2, Erk1/2, p-H2AX, H2AX, with β-Actin as a control. Levels of p-Mek1/2, Mek1/2, p-Erk1/2, Erk1/2, p-H2AX, H2AX, and β-Actin were quantified by densitometry. Levels of specific phosphorylation of Mek1/2 (p-Mek1/2/Mek1/2), Erk1/2 (p-Erk1/2/Erk1/2), and H2AX (p-H2AX/H2AX) were calculated by normalizing levels of p-Mek1/2, p-Erk1/2, and p-H2AX with levels of Mek1/2, Erk1/2, and H2AX, respectively, and then further normalizing with β-Actin level and the level set in untreated cells (lane 1) as 1 (X, arbitrary unit). All results are representative of three independent experiments.

**Figure 4.**

GTC intervention of carcinogen-induced gene expression. MCF10A cells were treated with combined NNK and B[a]P (NB) each at 100 pmol/L in the presence of 40 μ g/mL of GTC for 24 h. Total RNAs were isolated and analyzed by reverse transcription PCR with specific primers to determine relative gene expression levels of COX17, S100P, ATM, and TNFRSF8, with β -Actin as a control. Total gene expression levels of COX17, S100P, ATM, TNFRSF8, and β -Actin were quantified by densitometry. Relative gene expression levels were calculated by normalizing the levels of COX17, S100P, ATM, and TNFRSF8 gene expression with β -Actin level and the level set in untreated cells (lane1) as 1 (X, arbitrary unit). All results are representative of three independent experiments.

Table 1

Genes Up- and Down-regulated by NNK and B[a]P and Protected by GTC

Gene name	Function	Changes induced by NNK & B[a]P
Expression associated with ROS elevation		
BAX (BCL2-associated X protein)	Regulated by ROS via increasing promoter activity [56]	↑
COX17 (Cytochrome c oxidase assembly homolog-17)	Regulate ROS elevation by increasing activity of cytochrome oxidase [57]	↑
MRPL41 (Mitochondrial ribosomal protein L41)	Induced by ROS to help stabilize p53 [58]	↑
Expression associated with cell proliferation		
B4GALT1 (BetaGlcNAc beta 1,4-galactosyltransferase-1)	Increase proliferation by enhancing estrogen expression [59]	↑
BARHL1 (BarH-like homeobox-1)	Induce migration and survival of neural cells [60]	↑
BOLA3 (BoIA homolog-3)	Increase proliferation by regulating cell cycle [61]	↑
MT1E (Metallothionein 1E)	Induce proliferation and migration of bladder cancer cells [62]	↑
TNFRSF8 (Tumor necrosis factor receptor superfamily-8)	Decrease proliferation and increase apoptosis [63]	↓
Expression associated with ERK pathway activation		
S100P (S100 calcium binding protein P)	Regulate Erk phosphorylation in colon cancer cells [64]	↑
SPRR1B (Small proline-rich protein 1B)	Regulated by ERK pathway in epithelial cells [65]	↑
Expression associated with DNA damage		
ATM (Ataxia telangiectasia mutated)	Induced by double strand DNA damage [55]	↑
PER1 (Period homolog-1)	Induce DNA damage in human cancer cells [66]	↑

↑ up-regulation; ↓ down-regulation